

$\text{Ln}_3\text{Pb}_3(\text{IO}_3)_{13}(\mu^3\text{-O})$ (Ln = La–Nd): New Types of Second-Order Nonlinear Optical Materials Containing Two Types of Lone Pair Cations

Ting Hu,^{†,‡} Li Qin,^{†,‡} Fang Kong,^{†,‡} Yong Zhou,^{†,‡} and Jiang-Gao Mao^{*,†}

State Key Laboratory of Structural Chemistry, Fujian Institute of Research on the Structure of Matter, Chinese Academy of Sciences, Fuzhou 350002, P. R. China, and Graduate School of the Chinese Academy of Sciences, Beijing 100039, P. R. China

Received November 20, 2008

Hydrothermal reactions of lanthanide oxide, lead chloride, I_2O_5 , and H_2O at 200 °C led to four novel quaternary compounds, namely, $\text{Ln}_3\text{Pb}_3(\text{IO}_3)_{13}(\mu^3\text{-O})$ (Ln = La–Nd). They are isostructural, and their structures feature a complicated 3D network composed of LaO_9 and PbO_6 polyhedra interconnected by asymmetric IO_3 groups. $\text{Ln}_3\text{Pb}_3(\text{IO}_3)_{13}(\mu^3\text{-O})$ (Ln = La, Pr, Nd) display moderate second harmonic generation efficiencies of about 2.0, 1.0, and 0.8 times the value of KH_2PO_4 , respectively. These compounds are thermally stable up to 520 °C. Luminescence measurements indicate that $\text{Ln}_3\text{Pb}_3(\text{IO}_3)_{13}(\mu^3\text{-O})$ (Ln = Ce, Pr, Nd) exhibit strong emission bands in the visible or near IR region. Magnetic studies indicate that there exist significant antiferromagnetic interactions between magnetic centers in $\text{Ln}_3\text{Pb}_3(\text{IO}_3)_{13}(\mu^3\text{-O})$ (Ln = Pr, Nd).

Introduction

The search of new second-order nonlinear optical (NLO) material is of current interest and great importance owing to their applications in photonic technologies.¹ Currently, the most widely used such materials are inorganic crystals based on borates such as $\beta\text{-BaB}_2\text{O}_4$ and LiB_3O_5 and on phosphates such as KH_2PO_4 (KDP) and KTiOPO_4 .² It is reported that the π -conjugated system based on triangular BO_3 groups is responsible for the second harmonic generation (SHG) properties of the borates.^{1,3} Structurally, any NLO materials must have a noncentrosymmetric (NCS) structure. It is reported that inorganic compounds with asymmetric or polar coordination geometries are likely to display NCS structures and exhibit good SHG properties. Two such classes of cations are well-known: cations with stereochemically active lone pair electrons such as Se^{4+} and Te^{4+} and d^0 transition metals

(Ti^{4+} , Nb^{5+} , W^{6+} , etc.) in a distorted octahedral coordination environment, both of which are susceptible to second-order Jahn–Teller distortions (SOJT).⁴ The introduction of the lone pair cation $\text{Se}(\text{IV})$ into the borate system led to the discovery of a new type of SHG material.⁵ Furthermore, it has been demonstrated that the combination of the above two types of cations with the SOJT effect can lead to a number of compounds with excellent SHG properties as a result of the “additive” polarization of both types of bonds,^{6–9} as shown by BaTeM_2O_9 (M = Mo^{6+} or W^{6+}) and $\text{Na}_2\text{Te}_3\text{Mo}_3\text{O}_{16}$.^{7c,8e}

* To whom correspondence should be addressed. E-mail: mjg@fjirm.ac.cn.

[†] Fujian Institute of Research on the Structure of Matter, Chinese Academy of Sciences.

[‡] Graduate School of the Chinese Academy of Sciences.

- (1) (a) Chen, C.; Liu, G. *Annu. Rev. Mater. Sci.* **1986**, *16*, 203. (b) Ok, K. M.; Halasyamani, P. S. *Chem. Soc. Rev.* **2006**, *35*, 710.
- (2) (a) Becker, P. *Adv. Mater.* **1998**, *10*, 979. (b) Chen, C.-T.; Wang, Y.-B.; Wu, B.-C.; Wu, K.-C.; Zeng, W.-L.; Yu, L.-H. *Nature* **1995**, *373*, 322. (c) Chen, C.-T.; Wu, B.-C.; Jiang, A. D.; You, G. M. *Sci. Sin., Ser. B: Engl. Ed.* **1985**, *18*, 235. (d) Hagerman, M. E.; Poeppelmeier, K. R. *Chem. Mater.* **1995**, *7*, 602.
- (3) Pan, S. L.; Smit, J. P.; Watkins, B.; Marvel, M. R.; Stern, C. L.; Poeppelmeier, K. R. *J. Am. Chem. Soc.* **2006**, *128*, 11631.

- (4) (a) Halasyamani, P. S.; Poeppelmeier, K. R. *Chem. Mater.* **1998**, *10*, 2753. (b) Halasyamani, P. S. *Chem. Mater.* **2004**, *16*, 3586. (c) Ok, K. M.; Halasyamani, P. S. *Chem. Mater.* **2006**, *18*, 3176.
- (5) Kong, F.; Huang, S.-P.; Sun, Z.-M.; Mao, J.-G.; Cheng, W.-D. *J. Am. Chem. Soc.* **2006**, *128*, 7750.
- (6) (a) Porter, Y.; Bhuvanesh, N. S. P.; Halasyamani, P. S. *Inorg. Chem.* **2001**, *40*, 1172. (b) Porter, Y.; Ok, K. M.; Bhuvanesh, N. S. P.; Halasyamani, P. S. *Chem. Mater.* **2001**, *13*, 1910. (c) Ok, K. M.; Bhuvanesh, N. S. P.; Halasyamani, P. S. *Inorg. Chem.* **2001**, *40*, 1978.
- (7) (a) Porter, Y.; Halasyamani, P. S. *J. Solid State Chem.* **2003**, *174*, 441. (b) Harrison, W. T. A.; Dussack, L. L.; Jacobson, A. J. *Inorg. Chem.* **1994**, *33*, 6043. (c) Chi, E. O.; Ok, K. M.; Porter, Y.; Halasyamani, P. S. *Chem. Mater.* **2006**, *18*, 2070. (d) Balraj, V.; Vidyasagar, K. *Inorg. Chem.* **1998**, *37*, 4764.
- (8) (a) Kim, J.-H.; Baek, J.; Halasyamani, P. S. *Chem. Mater.* **2007**, *19*, 5637. (b) Goodey, J.; Broussard, J.; Halasyamani, P. S. *Chem. Mater.* **2002**, *14*, 3174. (c) Goodey, J.; Ok, K. M.; Broussard, J.; Hofmann, C.; Escobedo, F. V.; Halasyamani, P. S. *J. Solid State Chem.* **2003**, *175*, 3. (d) Harrison, W. T. A.; Dussack, L. L.; Jacobson, A. J. *J. Solid State Chem.* **1996**, *125*, 234. (e) Ra, H. S.; Ok, K. M.; Halasyamani, P. S. *J. Am. Chem. Soc.* **2003**, *125*, 7764.

Metal iodates also contain a lone pair cation I(V) in an asymmetric coordination geometry, and many of them are SHG-active.^{10–17} So far, a large number of ternary metal iodates have been reported; the cations used include alkali, alkaline earth, transition metal, lanthanide, and post-transition metal main group elements.^{10–12} A large number of actinide iodates [mostly U(VI) and Th(IV)] have been prepared by Albrecht-Schmitt group.^{13,14} Similar to metal selenites or tellurites, various SOJT d^0 transition metal ions have been introduced into the above ternary systems in search of materials with large SHG response.^{15–17} Like Te(IV), I(V) also exhibits several different coordination geometries such as IO_3 , IO_4 , and IO_5 , and they are able to polymerize into polynuclear anions with isolated cluster units such as I_3O_8^- or extended structures such as layered $\text{I}_4\text{O}_{11}^{2-}$ formed by asymmetric IO_5 and IO_3 polyhedra in $\alpha\text{-Cs}_2\text{I}_4\text{O}_{11}$ and pseudo-three-dimensional $\text{I}_4\text{O}_{11}^{2-}$ formed by asymmetric IO_4 and IO_3 polyhedra in $\beta\text{-Cs}_2\text{I}_4\text{O}_{11}$.¹⁰ We are especially interested in lanthanide iodates since they may also display useful luminescent properties in the UV, visible, or near IR regions.^{8a,b} So far, lanthanide iodates reported include

$\text{Ln}(\text{IO}_3)_3$ ($\text{Ln} = \text{La}–\text{Er}$, Yb , Sc), $\text{Ln}(\text{IO}_3)_3(\text{H}_2\text{O})$ ($\text{Ln} = \text{Yb}$, Lu), $\text{Ln}(\text{IO}_3)_3 \cdot 2\text{H}_2\text{O}$ ($\text{Ln} = \text{Eu}$, Gd , Dy , $\text{Er}–\text{Lu}$, Y), $\text{La}(\text{IO}_3)_3 \cdot 0.5\text{H}_2\text{O}$, $\text{Ln}(\text{MoO}_2)(\text{IO}_3)_4(\text{OH})$ ($\text{Ln} = \text{La}$, $\text{Nd}–\text{Eu}$), $\text{LaTiO}(\text{IO}_3)_5$, and $\text{NaYI}_4\text{O}_{12}$.^{10c,12,17} The Pb^{2+} cation has a large ionic radius and is able to exhibit several types of asymmetric coordination geometries as a result of the existence of stereochemically active lone pair electrons. We deem that the incorporation of such a cation into the lanthanide iodate systems may help the formation of new compounds with NCS structures and excellent optical properties. Guided by this idea, we prepared a series of new compounds, namely, $\text{Ln}_3\text{Pb}_3(\text{IO}_3)_{13}(\mu^3\text{-O})$ ($\text{Ln} = \text{La}–\text{Nd}$). These compounds display good SHG as well as luminescent properties. Herein, we report their syntheses, crystal structures, and optical properties.

Experimental Section

Materials and Methods. All of the chemicals were analytically pure from commercial sources and used without further purification. PbCl_2 and I_2O_5 were purchased from the Shanghai Reagent Factory (AR, 90.0+%) and La_2O_3 (99.99+%) was purchased from Ruikie National Engineering Research Centre of Rare Earth Metallurgy and Function Materials. IR spectra were recorded on a Magna 750 FT-IR spectrometer as KBr pellets in the range of 4000–400 cm^{-1} . Microprobe elemental analyses were performed on a field emission scanning electron microscope (FESEM, JSM6700F) equipped with an energy dispersive X-ray spectroscopy (EDS, Oxford INCA). X-ray powder diffraction (XRD) patterns were collected on a XPERT-MPD θ – 2θ diffractometer using graphite-monochromated $\text{Cu K}\alpha$ radiation in the range $2\theta = 5–85^\circ$ with a step size of 0.05°. Optical diffuse reflectance spectra were measured at room temperature with a PE Lambda 900 UV–visible spectrophotometer. A BaSO_4 plate was used as a standard (100% reflectance). The absorption spectrum was calculated from reflectance spectra using the Kubelka–Munk function: $\alpha/S = (1 - R)^2/2R$,¹⁸ where α is the absorption coefficient, S is the scattering coefficient which is practically wavelength independent when the particle size is larger than 5 μm , and R is the reflectance. Thermogravimetric analyses (TGA) were carried out with a NETZSCH STA 449C unit at a heating rate of 5 $^\circ\text{C}/\text{min}$ under a nitrogen atmosphere. Differential thermal analysis (DTA) was performed under N_2 on a NETZSCH DTA404PC. The sample and reference (Al_2O_3) were enclosed in Pt crucibles, heated from room temperature to 780 $^\circ\text{C}$, and then cooled to room temperature at a rate of 5 $^\circ\text{C}/\text{min}$. Photoluminescence analyses were performed on an Edinburgh FLS920 fluorescence spectrometer for the Nd compound or a Perkin-Elmer LS55 fluorescence spectrometer for other compounds. The measurements of the powder frequency-doubling effect was carried out on the sieved (80–100 mesh) powder samples of $\text{Ln}_3\text{Pb}_3(\text{IO}_3)_{13}(\mu^3\text{-O})$ ($\text{Ln} = \text{La}–\text{Nd}$) by means of the modified method of Kurtz and Perry.¹⁹ The fundamental wavelength is 1064 nm generated by a Q-switched Nd:YAG laser. The SHG wavelength is 532 nm. KDP powder sieved (80–100 mesh) was used as a reference to assume the effect. Magnetic susceptibility measurements on polycrystalline samples were performed with a PPMS-9T magnetometer at a field of 5000 Oe in the temperature range 2–300 K. The raw data were corrected for the susceptibility of the container and the diamagnetic contributions of the sample using Pascal's constants.²⁰

- (9) (a) Shen, Y. L.; Jiang, H. L.; Xu, J.; Mao, J. G.; Cheah, K. W. *Inorg. Chem.* **2005**, *44*, 9314. (b) Jiang, H. L.; Ma, E.; Mao, J. G. *Inorg. Chem.* **2007**, *46*, 7012. (c) Jiang, H. L.; Xie, Z.; Mao, J. G. *Inorg. Chem.* **2007**, *46*, 6495. (d) Jiang, H.-L.; Huang, S.-P.; Fan, Y.; Mao, J.-G.; Cheng, W.-D. *Chem.—Eur. J.* **2008**, *14*, 1972.
- (10) (a) Phanon, D.; Gautier-Luneau, I. *Angew. Chem., Int. Ed.* **2007**, *46*, 8488. (b) Ok, K. M.; Halasyamani, P. S. *Angew. Chem., Int. Ed.* **2004**, *43*, 5489. (c) Ok, K. M.; Halasyamani, P. S. *Inorg. Chem.* **2005**, *44*, 9353.
- (11) (a) Phanon, D.; Mosset, A.; Gautier-Luneau, I. *J. Mater. Chem.* **2007**, *17*, 1123. (b) Ngo, N.; Kalachnikova, K.; Assefa, Z.; Haire, R. G.; Sykora, R. E. *J. Solid State Chem.* **2006**, *179*, 3824. (c) Phanon, D.; Bentría, B.; Benbental, D.; Mosset, A.; Gautier-Luneau, I. *Solid State Sci.* **2006**, *8*, 1466.
- (12) (a) Chen, X.; Xue, H.; Chang, X.; Zang, H.; Xiao, W. *J. Alloys Compd.* **2005**, *398*, 173. (b) Assefa, Z.; Ling, J.; Haire, R. G.; Albrecht-Schmitt, T. E.; Sykora, R. E. *J. Solid State Chem.* **2006**, *179*, 3653. (c) Sykora, R. E.; Khalifah, P.; Assefa, Z.; Albrecht-Schmitt, T. E.; Haire, R. G. *J. Solid State Chem.* **2008**, *181*, 1867. (d) Douglas, P.; Hector, A. L.; Levason, W.; Light, M. E.; Matthews, M. L.; Webster, M. Z. *Anorg. Allg. Chem.* **2004**, *630*, 479. (e) Hector, A. L.; Henderson, S. J.; Levason, W.; Webster, M. Z. *Anorg. Allg. Chem.* **2002**, *628*, 198.
- (13) (a) Bean, A. C.; Campana, C. F.; Kwon, O.; Albrecht-Schmitt, T. E. *J. Am. Chem. Soc.* **2001**, *123*, 8806. (b) Bean, A. C.; Peper, S. M.; Albrecht-Schmitt, T. E. *Chem. Mater.* **2001**, *13*, 1266. (c) Ling, J.; Albrecht-Schmitt, T. E. *Inorg. Chem.* **2007**, *46*, 346. (d) Sykora, R. E.; Wells, D. M.; Albrecht-Schmitt, T. E. *Inorg. Chem.* **2002**, *41*, 2304. (e) Bray, T. H.; Beitz, J. V.; Bean, A. C.; Yu, Y.; Albrecht-Schmitt, T. E. *Inorg. Chem.* **2006**, *45*, 8251. (f) Bean, A. C.; Ruf, M.; Albrecht-Schmitt, T. E. *Inorg. Chem.* **2001**, *40*, 3959.
- (14) (a) Sykora, R. E.; McDaniel, S. M.; Wells, D. M.; Albrecht-Schmitt, T. E. *Inorg. Chem.* **2002**, *41*, 5126. (b) Bean, A. C.; Xu, Y.; Danis, J. A.; Albrecht-Schmitt, T. E. *Inorg. Chem.* **2002**, *41*, 6775. (c) Sykora, R. E.; Bean, A. C.; Scott, B. L.; Runde, W.; Albrecht-Schmitt, T. E. *J. Solid State Chem.* **2004**, *177*, 725. (d) Sullens, T. A.; Almond, P. M.; Byrd, J. A.; Beitz, J. V.; Bray, T. H.; Albrecht-Schmitt, T. E. *J. Solid State Chem.* **2006**, *179*, 1192. (e) Bean, A. C.; Albrecht-Schmitt, T. E. *J. Solid State Chem.* **2001**, *161*, 416.
- (15) (a) Sykora, R. E.; Ok, K. M.; Halasyamani, P. S.; Albrecht-Schmitt, T. E. *J. Am. Chem. Soc.* **2002**, *124*, 1951. (b) Sykora, R. E.; Ok, K. M.; Halasyamani, P. S.; Wells, D. M.; Albrecht-Schmitt, T. E. *Chem. Mater.* **2002**, *14*, 2741. (c) Sykora, R. E.; Wells, D. M.; Albrecht-Schmitt, T. E. *J. Solid State Chem.* **2002**, *166*, 442. (d) Chen, X.; Zhang, L.; Chang, X.; Xue, H.; Zang, H.; Xiao, W.; Song, X.; Yan, H. *J. Alloys Compd.* **2007**, *428*, 54.
- (16) (a) Ok, K. M.; Halasyamani, P. S. *Inorg. Chem.* **2005**, *44*, 2263. (b) Sykora, R. E.; Wells, D. M.; Albrecht-Schmitt, T. E. *Inorg. Chem.* **2002**, *41*, 2697.
- (17) (a) Shehee, T. C.; Sykora, R. E.; Ok, K. M.; Halasyamani, P. S.; Albrecht-Schmitt, T. E. *Inorg. Chem.* **2003**, *42*, 457. (b) Chen, X.; Chang, X.; Zang, H.; Xiao, W. *J. Alloys Compd.* **2005**, *396*, 255.

(18) Wendlandt, W. M.; Hecht, H. G. *Reflectance Spectroscopy*; Interscience: New York, 1966.

(19) Kurtz, S. W.; Perry, T. T. *J. Appl. Phys.* **1968**, *39*, 3798.

Table 1. Crystal Data and Structural Refinements for $\text{Ln}_3\text{Pb}_3(\text{IO}_3)_{13}(\mu^3\text{-O})$ ($\text{Ln} = \text{La-Nd}$)

	$\text{La}_3\text{Pb}_3\text{I}_{13}\text{O}_{40}$	$\text{Ce}_3\text{Pb}_3\text{I}_{13}\text{O}_{40}$	$\text{Pr}_3\text{Pb}_3\text{I}_{13}\text{O}_{40}$	$\text{Nd}_3\text{Pb}_3\text{I}_{13}\text{O}_{40}$
fw	3328.00	3331.63	3334.00	3343.99
space group	$R\bar{3}c$	$R\bar{3}c$	$R\bar{3}c$	$R\bar{3}c$
a (Å)	22.234(2)	22.132(3)	22.122(4)	22.011(1)
c (Å)	13.702(1)	13.613(2)	13.543(3)	13.555(2)
V (Å ³)	5866(1)	5775(1)	5740(2)	5687.1(9)
Z	6	6	6	6
D_{calcd} (g·cm ⁻³)	5.652	5.748	5.787	5.858
μ (mm ⁻¹)	26.459	27.096	27.511	28.020
GOF on F^2	1.061	1.082	1.112	1.050
R1, wR2 ($I > 2\sigma(I)$) ^a	0.0436, 0.1071	0.0320, 0.0912	0.0518, 0.1225	0.0504, 0.1345
R1, wR2 (all data)	0.0442, 0.1076	0.0342, 0.0920	0.0540, 0.1247	0.0511, 0.1358

^a $R1 = \sum |F_o| - |F_c| / \sum |F_o|$, $wR2 = \{\sum w[(F_o)^2 - (F_c)^2]^2 / \sum w[(F_o)^2]\}^{1/2}$.

Preparations of $\text{Ln}_3\text{Pb}_3(\text{IO}_3)_{13}(\mu^3\text{-O})$ ($\text{Ln} = \text{La-Nd}$). The four compounds were synthesized by a similar method. Single crystals of $\text{Ln}_3\text{Pb}_3(\text{IO}_3)_{13}(\mu^3\text{-O})$ ($\text{Ln} = \text{La-Nd}$) were prepared by the hydrothermal reactions of a mixture containing lanthanide(III) oxide or nitrate (for the Ce compound), PbCl_2 , I_2O_5 , and H_2O (10 mL for the La and Ce compounds; 4 mL for the Pr and Nd compounds) in a 23 mL Teflon lined stainless steel vessel at 200 °C for 4 (for the La and Pr compounds) or 5 (for the Ce and Nd compounds) days, and then cooled to 30 at 6 °C/h before switching off the furnace. The final pH values of the reaction systems are about 1.0. The loaded chemical compositions are La_2O_3 (0.200 g, 0.613 mmol), PbCl_2 (0.200 g, 0.719 mmol), and I_2O_5 (0.800 g, 2.4 mmol) for the La compound; $\text{Ce}(\text{NO}_3)_3 \cdot 6\text{H}_2\text{O}$ (0.280 g, 0.645 mmol), PbCl_2 (0.160 g, 0.576 mmol), and I_2O_5 (0.418 g, 1.251 mmol) for the Ce compound; Pr_2O_3 (0.100 g, 0.303 mmol), PbCl_2 (0.200 g, 0.719 mmol), and I_2O_5 (0.450 g, 1.35 mmol) for the Pr compound; and Nd_2O_3 (0.100 g, 0.297 mmol), PbCl_2 (0.200 g, 0.719 mmol), and I_2O_5 (0.450 g, 1.35 mmol) for the Nd compound. The crystals were isolated in a yield of about 56, 89, 74, and 72%, respectively, for the La, Ce, Pr, and Nd compounds, by washing the reaction product with deionized water, and then dried in air. The atomic ratios of Ln:Pb:I determined by EDS are 3.5:3.0:16.8 for the La compound, 3.9:3.0:19.7 for the Ce compound, 3.4:3.0:15.5 for the Pr compound, and 3.2:3.0:15.9 for the Nd compound, which are close to those determined from single crystal X-ray structural analyses. Their purities were confirmed by XRD powder diffraction studies (see Supporting Information). IR data (KBr, cm^{-1}) is as follows: 477(m) and 763(s) for the La compound, 477(m) and 763(s) for the Ce compound, 478(m) and 768(s) for the Pr compound, and 478(m) and 769(s) for the Nd compound (see Supporting Information).

Single-Crystal Structure Determination. Data collections for both compounds were performed on a Rigaku Mercury CCD diffractometer equipped with a graphite-monochromated Mo $K\alpha$ radiation ($\lambda = 0.71073$ Å) at 293 K. The data sets were corrected for Lorentz and polarization factors as well as for absorption by the multiscan method.^{21a} Both structures were solved by the direct methods and refined by full-matrix least-squares fitting on F^2 by SHELX-97.^{21b} All atoms were refined with anisotropic thermal parameters, except the O6 atom in the La, Pr, and Nd compounds, the O7 atom in the Pr compound, and O1 atoms in the Ce and Nd compounds, which were refined with isotropic thermal parameters. In all four compounds, the lead site was refined to be disordered over two (for La and Nd compounds) or three orientations (for Ce and Pr compounds) to eliminate the high residual peaks around

Table 2. Important Bond Lengths (Å) for $\text{Ln}_3\text{Pb}_3(\text{IO}_3)_{13}(\mu^3\text{-O})$ ($\text{Ln} = \text{La-Nd}$)^a

	La	Ce	Pr	Nd
Ln(1)-O(6)#1	2.444(14)	2.427(10)	2.411(16)	2.385(16)
Ln(1)-O(10)#2	2.473(12)	2.459(10)	2.453(16)	2.425(15)
Ln(1)-O(11)	2.479(13)	2.465(10)	2.470(15)	2.429(14)
Ln(1)-O(2)	2.480(13)	2.466(10)	2.474(17)	2.441(13)
Ln(1)-O(4)	2.502(13)	2.475(10)	2.490(17)	2.450(15)
Ln(1)-O(7)#3	2.543(14)	2.531(10)	2.513(16)	2.495(15)
Ln(1)-O(1)#4	2.560(14)	2.559(10)	2.537(17)	2.51(2)
Ln(1)-O(8)	2.591(13)	2.583(10)	2.588(17)	2.533(16)
Ln(1)-O(13)#5	2.753(15)	2.747(13)	2.698(17)	2.709(18)
Pb(1)-O(12)#6	2.475(15)	2.457(12)	2.496(17)	2.481(16)
Pb(1)-O(4)	2.502(11)	2.493(9)	2.523(16)	2.491(13)
Pb(1)-O(6)	2.635(14)	2.628(11)	2.62(2)	2.632(14)
Pb(1)-O(2)	2.662(13)	2.652(10)	2.639(15)	2.636(15)
Pb(1)-O(13)	2.699(16)	2.658(13)	2.656(16)	2.673(19)
Pb(1)-O(14)	2.799(15)	2.739(10)	2.777(15)	2.725(24)
I(1)-O(3)	1.814(19)	1.798(15)	1.781(19)	1.81(2)
I(1)-O(1)	1.815(16)	1.803(15)	1.81(2)	1.86(3)
I(1)-O(2)	1.852(13)	1.849(10)	1.831(15)	1.874(14)
I(2)-O(5)	1.787(15)	1.797(12)	1.794(16)	1.788(17)
I(2)-O(6)	1.814(14)	1.818(10)	1.799(17)	1.826(15)
I(2)-O(4)	1.832(12)	1.837(10)	1.811(16)	1.839(13)
I(3)-O(9)	1.784(15)	1.804(12)	1.765(19)	1.773(16)
I(3)-O(8)	1.793(13)	1.787(10)	1.803(17)	1.797(16)
I(3)-O(7)	1.839(13)	1.838(10)	1.827(15)	1.845(15)
I(4)-O(12)	1.806(12)	1.794(10)	1.786(16)	1.783(14)
I(4)-O(11)	1.815(13)	1.781(10)	1.790(16)	1.806(13)
I(4)-O(10)	1.821(12)	1.799(11)	1.793(16)	1.822(15)
I(5)-O(13)#7	1.812(14)	1.830(11)	1.878(18)	1.826(17)
I(5)-O(13)	1.812(14)	1.830(11)	1.878(18)	1.826(17)
I(5)-O(13)#4	1.812(14)	1.830(11)	1.878(18)	1.826(17)

^a Symmetry transformations used to generate equivalent atoms: (#1) $-x + y, z, z - 1/2$, (#2) $-y + 2/3, -x + 1/3, z - 1/6$, (#3) $-x + y + 1/3, -x + 2/3, z - 1/3$, (#4) $-y, x - y, z$, (#5) $x, x - y, z - 1/2$, (#6) $-y + 2/3, x - y + 1/3, z + 1/3$, and (#7) $-x + y, -x, z$.

$>7.0 \text{ e} \cdot \text{Å}^{-3}$. The occupancy factors of these orientations were allowed to be refined to have a sum occupancy factor of 1.0 and equal displacement parameters for each orientation. Such treatments gave good R and R1 factors as well as acceptable residual peaks for all four compounds. Crystallographic data and structural refinements for the four compounds are summarized in Table 1. Important bond distances are listed in Table 2.

More details on the crystallographic studies as well as atomic displacement parameters are given as Supporting Information.

Results and Discussion

Hydrothermal reactions of lanthanide oxide, lead(II) chloride, and I_2O_5 in water at 200 °C led to a series of new isostructural lanthanide(III) lead(II) iodates, $\text{Ln}_3\text{Pb}_3(\text{IO}_3)_{13}(\mu^3\text{-O})$ ($\text{Ln} = \text{La-Nd}$). These compounds display good thermal stability, moderate SHG response, and strong luminescence.

(20) Kahn, O. *Molecular Magnetism*; VCH Publishers, Inc.: New York, 1993; pp 3-4.

(21) (a) *CrystalClear*, Version 1.3.5; Rigaku Corp: Woodlands, TX, 1999. (b) Sheldrick, G. M. *SHELXTL, Crystallographic Software Package*, Version 5.1; Bruker-AXS: Madison, WI, 1998.

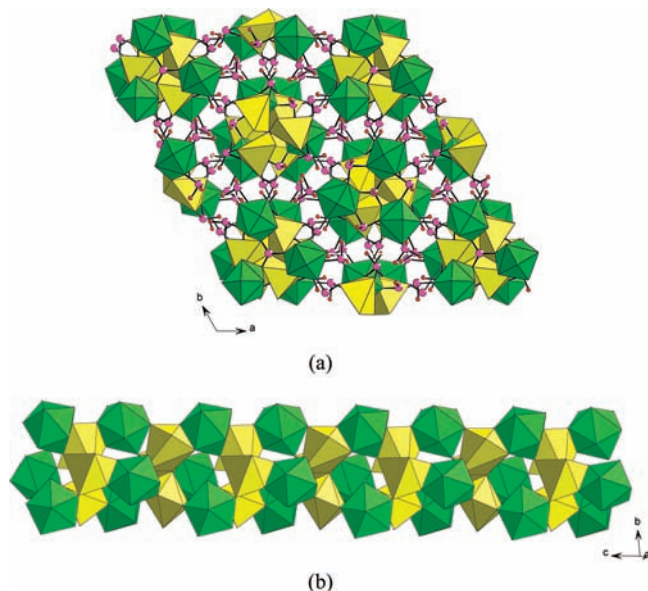


Figure 1. View of the structure of $\text{La}_3\text{Pb}_3(\text{IO}_3)_{13}(\mu^3\text{-O})$ down the c axis (a) and 1D chain formed by LaO_9 and PbO_6 polyhedra interconnected via edge and corner sharing. LaO_9 and PbO_6 polyhedra are shaded in green and yellow, respectively. I and O atoms are drawn as pink and red circles, respectively.

Structural Descriptions. The structures of $\text{Ln}_3\text{Pb}_3(\text{IO}_3)_{13}(\mu^3\text{-O})$ ($\text{Ln} = \text{La-Nd}$) exhibit a complicated three-dimensional network structure composed of LaO_9 , asymmetric PbO_6 , and IO_3 polyhedra that are interconnected via corner or edge sharing (Figure 1a). Since they are isostructural, only the structure of the lanthanum(III) compound will be discussed in detail as a representative.

There are one lanthanum(III) ion, one Pb(II) cation (distorted over two orientations, Pb1 and Pb1' with 81% and 19% occupancy factors, respectively), one O^{2-} anion, and five unique iodate groups in the asymmetric unit of $\text{La}_3\text{Pb}_3(\text{IO}_3)_{13}(\mu^3\text{-O})$. The $\mu^3\text{-O}^{2-}$ anion (O14) and I(5) atom are located at sites with a C_3 symmetry, whereas all other remaining atoms occupy general positions. The La^{3+} ion is bonded to nine oxygen atoms from nine iodate anions in a tricapped trigonal-prismatic environment (Figure 2b). The La-O bond distances range from 2.444(14) to 2.753(15) Å, which are comparable to those reported in other lanthanum(III) iodates.^{12,17} All five unique I^{5+} cations are asymmetrically coordinated by three oxygen atoms in a distorted trigonal-pyramidal environment; the I-O bond distances are in the range of 1.784(15)–1.852(13) Å. Pb1 is six-coordinated by six oxygens in a severely distorted PbO_6 octahedral geometry because of the presence of the lone pair of the Pb(II) ion. The Pb-O distances range from 2.475(15) to 2.799(15) Å; these distances are comparable to those reported in other lead(II) iodate.²²

The structure of $\text{La}_3\text{Pb}_3(\text{IO}_3)_{13}(\mu^3\text{-O})$ can also be viewed as based on 1D columns composed of LaO_9 and PbO_6 polyhedra interconnected via corner and edge sharing (Figure 1b). I(5) atoms occupy the voids of the columns, as such columns are further interconnected by bridging $\text{I}(1)\text{O}_3$,

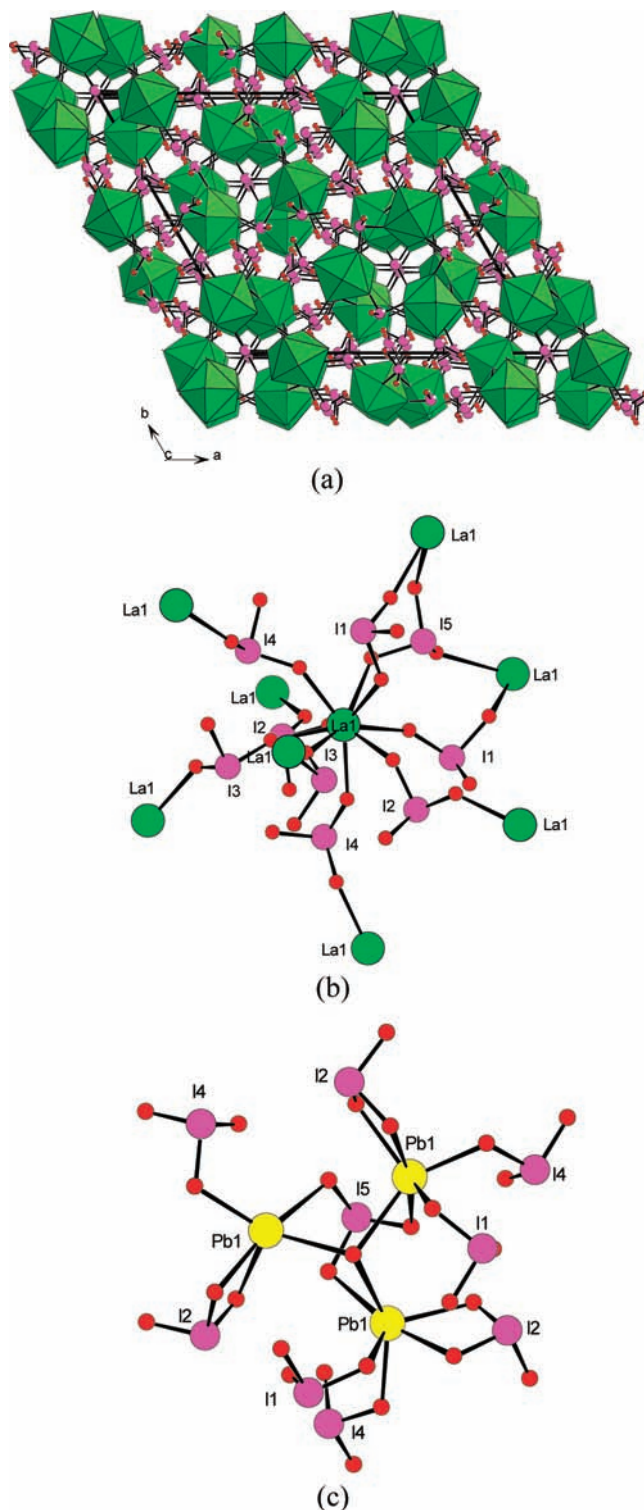


Figure 2. 3D network of lanthanum(III) iodate (a), connectivity between La(III) ions and iodate anions (b), and trinuclear lead(II) iodate (c) in $\text{La}_3\text{Pb}_3(\text{IO}_3)_{13}(\mu^3\text{-O})$. LaO_9 polyhedra are shaded in green. La, Pb, I, and O atoms are drawn as green, yellow, pink, and red circles, respectively.

$\text{I}(2)\text{O}_3$, $\text{I}(3)\text{O}_3$, and $\text{I}(4)\text{O}_3$ groups in a 3D architecture. The O^{2-} anion (O14) is tridentate and bridges with three $\text{Pb1}'$ atoms with a Pb-O distance of 2.312(16) Å; it also forms three longer Pb-O bonds (2.799(15) Å) with three Pb1 atoms.

It is interesting to note that the interconnection of LaO_9 polyhedra by bridging iodate anions resulted in a 3D network

(22) Kellersohn, T.; Alici, E.; Esser, D.; Lutz, H. D. *Z. Kristallogr.* **1993**, *203*, 225.

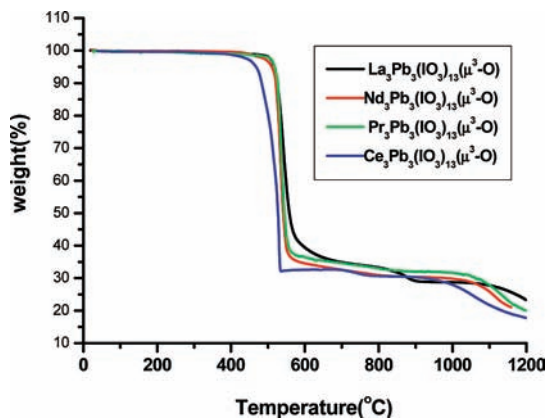


Figure 3. TGA curves for $\text{Ln}_3\text{Pb}_3(\text{IO}_3)_{13}(\mu^3\text{-O})$ ($\text{Ln} = \text{La-Nd}$).

(Figure 2a), whereas three Pb(1) atoms are bridged by the $\text{I}(5)\text{O}_3$ group as well as an O(14) atom in a trinuclear unit with the remaining coordination sites filled by $\text{I}(1)\text{O}_3$, $\text{I}(2)\text{O}_3$, and $\text{I}(4)\text{O}_3$ anions in a unidentate fashion (Figure 2c). Within the 3D network of the lanthanum(III) iodate, the $\text{I}(5)\text{O}_3$ group bridges with three La(III) ions, whereas with the remaining IO_3 groups, each bridges with two La(III) centers (Figure 2b).

It is also worthy to compare the structure of $\text{La}_3\text{Pb}_3(\text{IO}_3)_{13}(\mu^3\text{-O})$ with those of $\text{La}(\text{IO}_3)_3$ and $\text{Pb}(\text{IO}_3)_2$.^{10c,22} $\text{La}(\text{IO}_3)_3$ in the monoclinic space group *Cc* exhibits a SHG response of $400\times \text{SiO}_2$. Its structure features a 3D network that consists of LaO_9 polyhedra interconnected by the asymmetric IO_3 groups. Three LaO_9 polyhedra form a trimer by edge sharing.^{10c} $\text{Pb}(\text{IO}_3)_2$ is centrosymmetric (space group *Pbcn*), and its structure features a 1D chain of edge sharing asymmetric PbO_4 polyhedra with asymmetric IO_3 groups hanging on both sides of the chain.²²

Results of bond valence calculations indicate that the La, Pb, and I atoms are in an oxidation state of +3, +2, and +5, respectively. The calculated total bond valences are 3.45, 1.56, 4.80, 5.01, 5.09, 4.96, and 4.99, respectively, for La(1), Pb(1), I(1), I(2), I(3), I(4), and I(5).²³ The deviation of the value for the Pb(II) ion indicates that additional weak Pb–O bonds should be also included in the bond valence calculations, which is very common for lead(II) compounds.

Thermal Stability Studies. TGA studies indicate that $\text{Ln}_3\text{Pb}_3(\text{IO}_3)_{13}(\mu^3\text{-O})$ ($\text{Ln} = \text{La-Nd}$) are thermally stable up to about 552, 467, 541, and 529 °C respectively for La, Ce, Pr, and Nd compounds (Figure 3). Then, each displays one main step of weight loss. The sharp weight loss corresponds to the decomposition of the compound through thermal disproportionation, releasing 6.5 molecules of I_2 and 16.25 molecules of O_2 . The weight losses of 62.8% at 638 °C for the La compound, 67.6% at 532 °C for the Ce compound, 62.2% at 567 °C for the Pr compound, and 63.9% at 564 °C for the Nd compound are close to the calculated values of 62.3, 62.7, 65.1, and 64.9%. Upon further heating, there is a slight weight loss which may be due to the release of some volatile substances. The final residuals were not characterized because of their melting with the TGA bucket

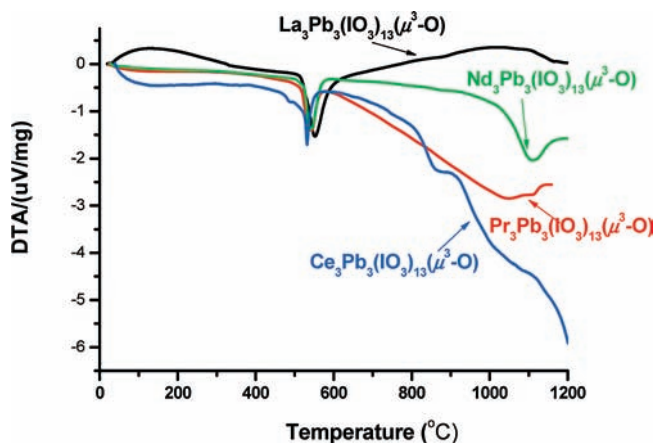


Figure 4. DTA curves for $\text{Ln}_3\text{Pb}_3(\text{IO}_3)_{13}(\mu^3\text{-O})$ ($\text{Ln} = \text{La-Nd}$).

made of Al_2O_3 under such high temperature. DTA diagrams of $\text{Ln}_3\text{Pb}_3(\text{IO}_3)_{13}(\mu^3\text{-O})$ ($\text{Ln} = \text{La-Nd}$) exhibit an endothermic peak at 553, 531, 540, and 540 °C, respectively, for the La, Ce, Pr, and Nd compounds in the heating curve (Figure 4), which is in good agreement with the results of the TGA analyses.

Optical Properties. IR studies indicate that the $\text{Ln}_3\text{Pb}_3(\text{IO}_3)_{13}(\mu^3\text{-O})$ ($\text{Ln} = \text{La-Nd}$) are transparent in the range of $4000\text{--}1000\text{ cm}^{-1}$ ($2.5\text{--}10.0\text{ }\mu\text{m}$; see Supporting Information). The IR absorption bands at $477\text{--}478\text{ cm}^{-1}$ and $763\text{--}769\text{ cm}^{-1}$ are due to the I–O vibrations. The UV absorption spectrum measurements indicate that both $\text{La}_3\text{Pb}_3(\text{IO}_3)_{13}(\mu^3\text{-O})$ and $\text{Ce}_3\text{Pb}_3(\text{IO}_3)_{13}(\mu^3\text{-O})$ show little absorption in the range of 600–1200 nm whereas $\text{Pr}_3\text{Pb}_3(\text{IO}_3)_{13}(\mu^3\text{-O})$ displays characteristic sharp absorption bands at 448, 474, 488, and 596 nm of the Pr(III) ion. $\text{Nd}_3\text{Pb}_3(\text{IO}_3)_{13}(\mu^3\text{-O})$ also exhibits characteristic sharp absorption bands at 433, 471, 526, 583, 628, 683, 746, 800, and 875 nm (see Supporting Information). These absorption bands are due to the f–f or f–d transition of the Pr^{3+} and the Nd^{3+} ions.²⁴

Optical diffuse reflectance spectrum studies indicate that $\text{Ln}_3\text{Pb}_3(\text{IO}_3)_{13}(\mu^3\text{-O})$ ($\text{Ln} = \text{La-Nd}$) revealed optical band gaps of 4.02, 2.4, 3.85, and 3.53 eV respectively for the La, Ce, Pr, and Nd compounds (Figure 5). The large differences of the band gaps for these isostructural compounds are mainly due to different electronic configurations for the lanthanide(III) ions.

Solid state luminescent spectra of $\text{Ln}_3\text{Pb}_3(\text{IO}_3)_{13}(\mu^3\text{-O})$ ($\text{Ln} = \text{Ce, Pr, Nd}$) were studied at room temperature (Figure 6). Upon excitation at 290 nm, $\text{Ce}_3\text{Pb}_3(\text{IO}_3)_{13}(\mu^3\text{-O})$ displays two strong emission bands at 438 and 466 nm, corresponding to the transition of 5d excited state to $^2\text{F}_{5/2}$ and $^2\text{F}_{7/2}$ of the cerium(III) ion (Figure 6a).²⁵ $\text{Pr}_3\text{Pb}_3(\text{IO}_3)_{13}(\mu^3\text{-O})$ displays four sets of emission bands at 487 nm (very strong, $^3\text{P}_0 \rightarrow ^3\text{H}_4$), 528 nm (moderate, $^3\text{P}_0 \rightarrow ^3\text{H}_5$), 612 nm (moderate, $^3\text{P}_0 \rightarrow ^3\text{H}_6$), 644 nm (strong, $^3\text{P}_0 \rightarrow ^3\text{F}_2$), and 729 nm (weak, $^3\text{P}_0 \rightarrow ^3\text{F}_4$) under $\lambda_{\text{ex}} = 448\text{ nm}$ (Figure 6b).^{9b} Under excitation

(24) Kaminskii, A. A. *Phys. Status Solidi* **1985**, *87*, 11.

(25) (a) Weis, E. M.; Bares, C. L.; Duval, P. B. *Inorg. Chem.* **2006**, *45*, 10126. (b) Vogler, A.; Kunkely, H. *Inorg. Chim. Acta* **2006**, *359*, 4130. (c) Yu, R.; Wang, J.; Zhang, J.; Yuan, H.; Su, Q. *J. Solid State Chem.* **2008**, *181*, 658.

(23) (a) Brown, I. D.; Altermatt, D. *Acta Crystallogr.* **1985**, *41*, 244. (b) Brese, N. E.; O’Keeffe, M. *Acta Crystallogr.* **1991**, *47*, 192.

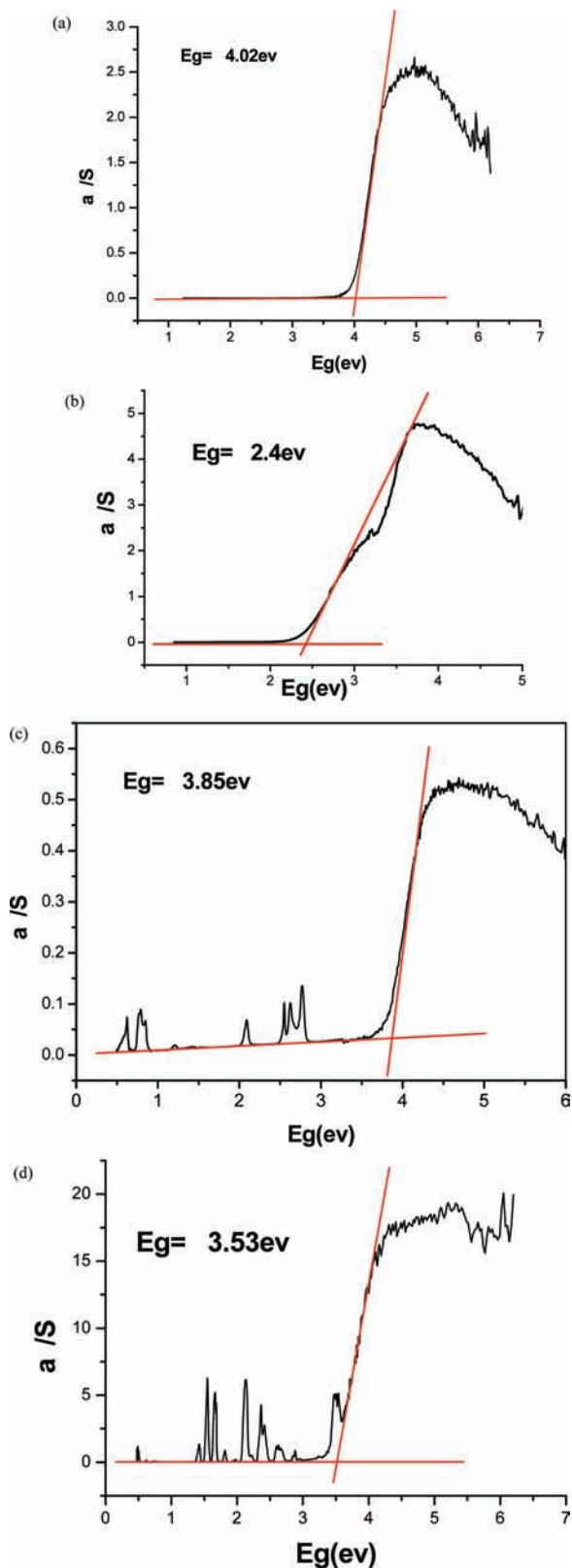


Figure 5. Optical diffuse reflectance spectra for $\text{La}_3\text{Pb}_3(\text{IO}_3)_{13}(\mu^3\text{-O})$ (a), $\text{Ce}_3\text{Pb}_3(\text{IO}_3)_{13}(\mu^3\text{-O})$ (b), $\text{Pr}_3\text{Pb}_3(\text{IO}_3)_{13}(\mu^3\text{-O})$ (c), and $\text{Nd}_3\text{Pb}_3(\text{IO}_3)_{13}(\mu^3\text{-O})$ (d).

at 524 nm, $\text{Nd}_3\text{Pb}_3(\text{IO}_3)_{13}(\mu^3\text{-O})$ displays three sets of emission bands, which are characteristic for the Nd(III) ion in the near IR region: a moderate emission band at around 893 nm (${}^4\text{F}_{3/2} \rightarrow {}^4\text{I}_{9/2}$), a very strong emission band at 1063

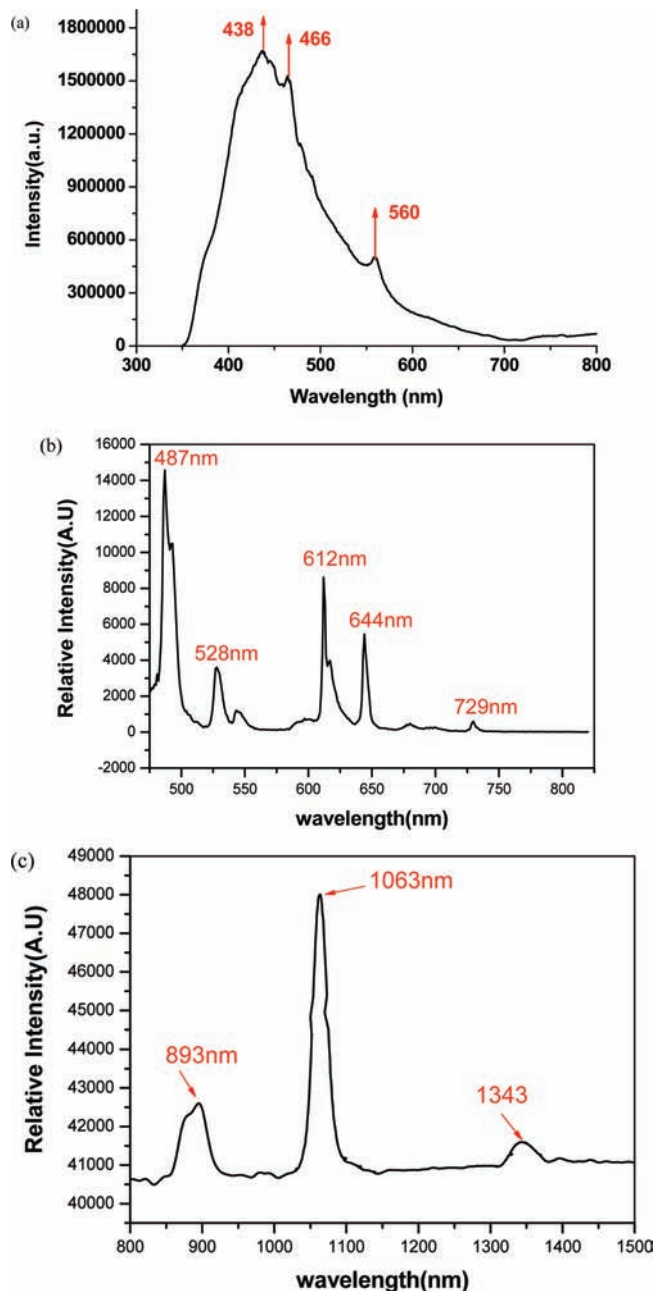


Figure 6. Solid state emission spectra of $\text{Ce}_3\text{Pb}_3(\text{IO}_3)_{13}(\mu^3\text{-O})$ under $\lambda_{\text{ex}} = 290$ nm (a), $\text{Pr}_3\text{Pb}_3(\text{IO}_3)_{13}(\mu^3\text{-O})$ under $\lambda_{\text{ex}} = 448$ nm (b), and $\text{Nd}_3\text{Pb}_3(\text{IO}_3)_{13}(\mu^3\text{-O})$ under $\lambda_{\text{ex}} = 524$ nm (c).

nm (${}^4\text{F}_{3/2} \rightarrow {}^4\text{I}_{11/2}$), and a weak band at about 1343 nm (${}^4\text{F}_{3/2} \rightarrow {}^4\text{I}_{13/2}$; Figure 6c).^{9a,b} The lifetime of the Nd (${}^4\text{F}_{3/2}$) state for $\lambda_{\text{ex, em}} = 524, 1060$ nm is measured to be about 3.8 μs .

SHG Measurements. $\text{Ln}_3\text{Pb}_3(\text{IO}_3)_{13}(\mu^3\text{-O})$ (Ln = La–Nd) crystallized in the acentric space group $R3c$. Hence, it is worthy to study their SHG properties. SHG measurements on a Q-switched Nd:YAG laser with the sieved powder sample (80–100 mesh) revealed that $\text{Ln}_3\text{Pb}_3(\text{IO}_3)_{13}(\mu^3\text{-O})$ (Ln = La, Pr, Nd) display SHG signals that about 2.0, 1.0, and 0.8 times of KDP, respectively. Unfortunately, the SHG signal for the cerium(III) compound is very weak. So far, we still cannot understand why its SHG response is not as strong as those for other lanthanide(III) analogues; however, we suspect that the Ce sample may be not phase-matching

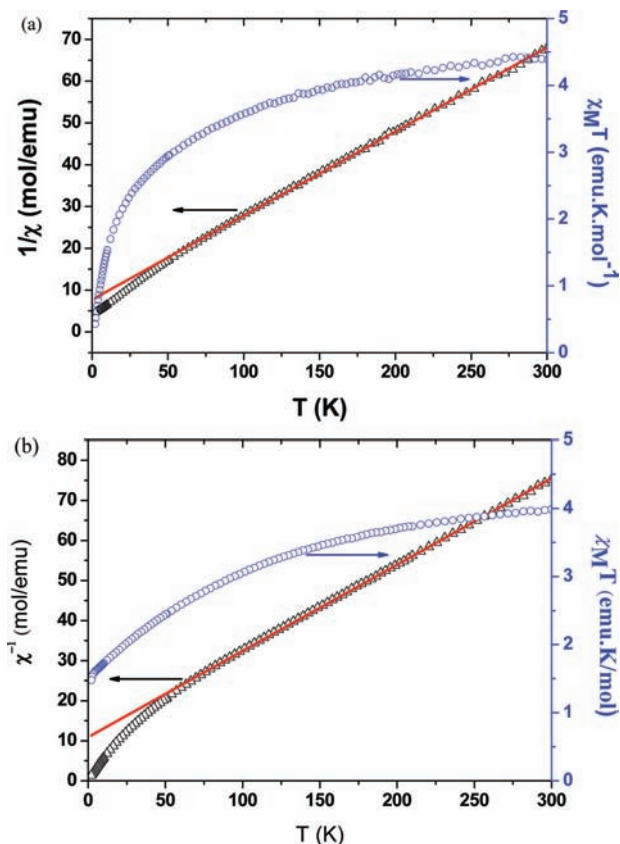


Figure 7. Plots of χ_m^{-1} versus temperature (T) of $\text{Pr}_3\text{Pb}_3(\text{IO}_3)_{13}(\mu^3\text{-O})$ (a) and $\text{Nd}_3\text{Pb}_3(\text{IO}_3)_{13}(\mu^3\text{-O})$ (b). The red line represents the linear fit of data according to the Curie–Weiss Law.

or of much poorer crystallinity. On the basis of structural data, it is expected that the polarization contributions of the $\text{Pb}(\text{II})$ ions and $\text{I}(1)\text{O}_3$, $\text{I}(2)\text{O}_3$, and $\text{I}(4)\text{O}_3$ groups are small since their dipole moments are mainly aligned in the ab plane, which canceled each other. The main polarization contributions are from $\text{I}(5)\text{O}_3$ and $\text{I}(3)\text{O}_3$ groups since their dipole moments are aligned in the same directions (along the c axis; see Supporting Information).

Magnetic Property Measurements. Magnetic properties for $\text{Ln}_3\text{Pb}_3(\text{IO}_3)_{13}(\mu^3\text{-O})$ ($\text{Ln} = \text{Pr}, \text{Nd}$) have been studied at a magnetic field of 5000 Oe in the temperature range of 2–300 K. The plots of $\chi_m T$ and χ_m^{-1} versus temperature (T) are shown in Figure 7. Both compounds obey the Curie–Weiss law in the range 50–300 K. At 300 K, the effective magnetic moments (μ_{eff}) are calculated to be 5.92 and 5.65 μ_B , respectively, for the Pr and Nd compounds, which are slightly smaller than the theoretical values (6.27 and 6.37 μ_B , respectively) for three isolated Ln(III) ions per formula unit. Upon cooling, the μ_{eff} values decreased and reached 1.86 and 3.44 μ_B at 2 K respectively for the Pr and Nd compounds,

indicating antiferromagnetic interactions between magnetic centers. Linear fitting of χ_m^{-1} data with T above 100 K gave Weiss constants of -38.4 and -50.7 K respectively for the Pr and Nd compounds. It should be noted that the Weiss constants for the Nd(III) compound are much more negative than those of the Pr(III) compound. Because the $\text{Pb}(\text{II})$, O^{2-} , and IO_3^{2-} anions are diamagnetic, the paramagnetic contributions of both compounds are expected to come solely from the Ln^{3+} ions. The magnetic interactions are expected to occur between Ln(III) ions interconnected through Ln–O–I–O–Ln bridges. The shortest Ln \cdots Ln separations are 6.977 and 6.952 Å for the Pr and Nd compounds, respectively. These data could explain most of the Weiss constants observed. More detailed calculations of these magnetic interactions were not performed because of the complexity of the structures as well as the lack of suitable models.

Conclusions

In summary, a series of novel quaternary lanthanide(III) lead(II) mixed metal iodates, namely, $\text{Ln}_3\text{Pb}_3(\text{IO}_3)_{13}(\mu^3\text{-O})$ ($\text{Ln} = \text{La-Nd}$), have been prepared and characterized. These compounds are isostructural and feature a complicated 3D network constructed by LaO_9 and PbO_6 polyhedra interconnected by the asymmetric IO_3 groups. More importantly, La, Pr, and Nd compounds exhibit good SHG properties, and they are thermally stable up to 520 °C. $\text{Ln}_3\text{Pb}_3(\text{IO}_3)_{13}(\mu^3\text{-O})$ ($\text{Ln} = \text{Ce}, \text{Pr}, \text{Nd}$) also display strong emission bands in the visible or near IR region. Results of our studies indicate that, by the introduction of the lone pair cation with large ionic size such as Pb^{2+} into the lanthanide iodate system, we can design new types of second-order NLO materials with high thermal stability. If the above two types of asymmetric units are properly aligned, it is expected that new NCS compounds with enhanced SHG response can be obtained. Our future research efforts will be devoted to the exploration of new SHG compounds by introduction of other large size lone pair cations such as Sn^{2+} and Bi^{3+} ions into the lanthanide iodates.

Acknowledgment. This work was supported by National Natural Science Foundation of China (Nos. 20731006, 20825104, and 20821061), the Knowledge Innovation Program of the Chinese Academy of Sciences, and the Key Project of FJIRSM (No. SZD07001-2). We thank Prof. Ding Li for his great help with the SHG measurements.

Supporting Information Available: X-ray crystallographic files in CIF format, simulated and experimental XRD patterns, and IR and UV absorption spectra for the four compounds. This material is available free of charge via the Internet at <http://pubs.acs.org>.

IC8022375